Uniosun Journal of Engineering and Environmental Sciences (UJEES), Vol. 8 No. 1, March, 2026
DOI: 10.64980/ujees.v8i1.010 **O. S. Teniola**
Published: March 30, 2026

OPTIMIZING THE ADSORPTION OF GOLD FROM DILUTE AQUA-REGIA-GOLD LEACHATE ONTO SUGARCANE BAGASSE GEL

O. S. TENIOLA[1*]
[1]*Department of Mechanical and Mechatronics Engineering, Abiola Ajimobi University, Ibadan, Nigeria.*

[*]*Corresponding Author: oluwasanmi.teniola@tech-u.edu.ng*

Abstract
An investigation was conducted on the adsorption behavior of gold (III) ions from a dilute aqua-regia leached solution of low-grade gold ore utilizing sugarcane bagasse gel. The experiment was designed using center composite design (CCD) with RSM, from which a quadratic model was created for regression analysis. Agitation rate, adsorbent concentration, contact time, and temperature are significant factors whose impacts were taken into account; their corresponding optimal values were determined to be 45 rpm, 1.4 g/L, 99 minutes, and 60°C. It was discovered that the adsorption yield was 91.5%. Additionally, it was discovered that the adsorption yield was 93.25% when analar grade activated carbon was utilized for the adsorption under ideal circumstances. The equilibrium sorption of Au(III) ions was performed at the ideal temperature of 323K. The results were fitted into Freundlich, Temkin, and Langmuir isotherms; the Langmuir model showed the best agreement with the experimental data.

Keywords
Aqua-regia, Refractory gold, Adsorption, bagasse, Isotherm

1. INTRODUCTION

With only 0.005 parts per million in the earth's crust, gold is a rare element that needs to be upgraded by a factor of 3000 to 4000 in order to reach commercial concentrations [1]. High cyanide consumption is typically necessary for the cyanidation of refractory gold ore, and the tailings of Refractory gold ore cyanidation typically necessitates considerable cyanide consumption, making it more challenging to discharge tailings of highly concentrated cyanide solution, which is typically higher than the extremely low allowed level of <0.1 ppm [2]. It has been discovered that aqua regia produces a potent oxidizing environment that can quickly dissolve free gold as well as the precarious sulfides and carbonaceous compounds [3]. A number of techniques, including precipitation, solvent extraction, ion-exchange, and adsorption, could be used to concentrate and separate the gold metals. Solvent extraction and precipitation are appropriate methods for recovering from highly concentrated solutions. Ion-exchange and adsorption work well in solutions with trace or low concentrations.

Gold recovery through adsorption from leach solution has been extensively accomplished using activated carbon. Activated carbon is typically not used for quantitative gold recovery, and traces of gold are usually retained in the solution [4]. A variety of biomass materials, including polysaccharides, cotton, paper, and biomass wastes, have been used to create bioadsorbents. Adsorbents produced from these sources have been used to recover gold (III), and it has been noted that they are very selective for gold over other metals [5].

There is a good chance that adsorption gel made from sugarcane (Saccharum Officinarum) bagasse using straightforward techniques will selectively adsorb gold (III) ions from aqua-regia leached solution, making the process of recovering gold from refractory gold ore more profitable. In order to maximize the adsorption of gold from diluted aqua-regia-gold leachate onto synthetic sugarcane bagasse gel, this study aims to determine the exact process parameters.

2. MATERIALS AND METHOD

2.1. Materials and Reagents

The gold ore sample was obtained directly from the Imogbara village mining site in Iperindo town, which is situated in the Atakumosa Local Government Area of Osun State, Nigeria. Panning in a flowing river nearby the mining site allowed the ore sample to be pre-concentrated. After washing, panned ore was extensively blended to ensure homogeneity [6]. The dried material was crushed using a Pascal Engineering crushing mill, model number 18862, which operated at 415 V, 2200 W, 4.9 A, and 50 Hz [7]. Using a pulverizer and a 75

µm sieve, a working sample size of 1 kg was obtained using the random sampling method, followed by the cone and quartering sampling method. Afterwards, the material was ground up and sieved until 80% passing had been obtained. X-ray fluorescence (XRF) was used to analyze the ore sample's chemical composition [8]; the results are shown in Table 1. For the leaching procedure and bagasse adsorption gel preparation, analar-grade hydrochloric acid, nitric acid, and sulfuric acid were utilized. Sugarcane bagasse was gathered from a nearby juice shop in Ogun State's Papalanto neighborhood.

Table 1: Chemical Composition of Gold-Bearing Rock Ore Using XRF.

Composition	Ppm
K	14452.59
Se	168.23
Rb	2781.25
Ti	5863.56
Pb	1113.48
Fe	274874.88
Ca	3529.31
S	Sr 1629.78
Sr	73.48
Th	462.38
As	266.13
Ag	0.86
Mo	239.77
Au	113.78
Zn	4407.29
Ni	1264.57
Co	1374.97
Mn	14076.40
Cr	1707.55
V	449.37

2.2. Aqua-Regia Agitated Leaching

The pulverized refractory gold ore was subjected to agitated leaching utilizing a modified [9] technique. A glass reactor with 50 milliliters of prepared aqua regia solution was filled with 5 grams of the ore sample. The reactor was covered and shook for three minutes after the stirrer was added. After that, the reactor was put on a magnetic stirrer plate with a temperature of 90°C and a speed of 300 rpm. After the two hours of leaching, the mixture was allowed to cool before being filtered out using Whatmann filter paper. Atomic Absorption Spectrometry (AAS) Perkin Elmer 1100BAAS with a graphite furnace and HGA (high graphite atomization) 700 was used to assess the filtrate's gold content. Following each leaching test, the concentration of gold in the leaching solution was 1.8–2 ppm.

2.3. Preparation of Bagasse Gel

A modified approach from [10 was used to extract bagasse gel. After being cleaned of all impurities, the collected bagasse was oven-dried for a whole night at 110°C. The dried sample was put in a ceramic crucible and heated to 600°C in a muffle furnace. The crucible was taken out after two hours of roasting, and the bagasse ash inside was let to cool to room temperature. By leaching 10 g of bagasse ash with 100 ml of 1 M HCl for 30 minutes, heavy metals were extracted from the ash. The leached ash was cleaned with distilled water and then refluxed for two hours in 100 milliliters of 3 M NaOH. The resultant solution was filtered to get rid of the suspended solid particles and basically contained sodium silicate. The clear solution was then titrated with 3 M HCl until the pH reached 5, which is when silica gel precipitation starts. For six hours, the gel was aged [11]. Centrifugation was used to separate the silica gel, and it was then rinsed until the aqueous portion reacted negatively with chloride.

2.4. Gold Adsorption Test

Following aqua-regia leaching, gold cation adsorption was performed using the [12] approach. The prepared sugarcane bagasse gel was used for the adsorption process. An Erlenmeyer flask was used for the experiment. A 20 ml sample of gold leachate containing Au3+ was mixed with around 0.5 g of the adsorbent. For different times and temperatures, the flask was set on a magnetic stirrer hot plate. After that, the phases were separated by filtration, and atomic absorption spectrometry was used to determine how much cation was still present in the leachate.

The percentage of ion uptake was calculated using equations 1

$$uptake\% = \frac{(C_o - C_e)}{C_o} X100 \quad (1)$$

where C_o and C_e are the initial and equilibrium concentration of ions (mg L^{-1}), respectively.

Furthermore, equation 2 was used to compute the adsorption capacity of gold (III) in order to estimate the kinetics and equilibrium studies.

$$q_x = \frac{(C_i - C_e)}{m} XV \quad (2)$$

Where V (ml) and m (mg) are the volume of the gold ion solution and the weight of adsorbent, respectively.

The factors that influence gold adsorption that were studied include contact time (30, 60, 90 and 120 mins), temperatures (30, 40, 50 and 60ºC), adsorbent concentration (0.5, 0.75, 1, 1.25, 1.5 g/L) and agitation rate (35, 40, 45, 50, 55 rpm). The procedure described was repeated for the best condition using the traditional activated carbon as the adsorbent, to facilitate efficiency comparison.

2.5. Design of Adsorption Experiment using RSM and Data Analysis

Using Design Expert Centre Composite Design (CCD), an exploratory plan was created to examine and optimize the impact of a few key factors on gold adsorption and recovery [13]. Four elements—temperature, stirring speed, mass of adsorbent, and contact time—each at five levels (-2, -1, 0, +1, +2) were chosen (TABLE 2).

Table 2: The factors affecting the adsorption process of gold and their levels.

Factor	Symbol	Factorial levels			Star point (α = 2.0)	
		Low (-1)	Centre (0)	High (+1)	-2	+2
Mass of adsorbent	A	0.6	1.05	1.5	0.15	1.95
Contact time	B	60	90	120	30	150
Temperature	C	39	56	73	22	90
Agitation	D	40	45	50	35	55

3. RESULTS AND DISCUSSION

3.1. Building empirical model and statistical analysis

It is first necessary to choose a model that will be used to describe the behavior of the selected factors on the gold adsorption rate. Hence, experimental data in TABLE 3 were fitted with various mathematical models, such as linear, two factorial interaction (2FI), quadratic and cubic. Data collected from various mathematical models (Linear, 2FI, quadratic and cubic) as well as analysis of variance (ANOVA) proved that the adsorption rate of gold on nanocellulose synthesized from sugarcane bagasse was most suitably described with a quadratic polynomial model in the following form (Eq. 3)

$$R = \beta_o + \sum_{i=1}^{k} \beta_i x_i + \sum_{i=1}^{k} \beta_{ii} x_i^2 + \sum_{1 \le i \le j}^{k} \beta_{ij} x_i x_j + \varepsilon \quad (3)$$

Where k, βo, βi, xi, xj, βii, βij and ε represent the number of variables, a constant term, the coefficients of the linear parameters, the variables, the coefficients of the quadratic parameter, the coefficients of the interaction parameters and the residual associated with the experiments, respectively. The final equation representing the

gold adsorption rate (R) in terms of coded factors was obtained as functions of mass of adsorbent (A), contact time (B), temperature (C) and agitation (D) is presented in eq. (4).

$$R = 82.05 + 19.19A + 5.75B + 0.065C - 0.3742D - 3.16AB + 0.8888AC + 0.1288AD - 0.6475BC - 0.1850BD + 0.5988CD - 8.59A^2 - 2.64B^2 - 7.58C^2 - 0.8429D^2 \quad (4)$$

Table 3: CCD matrix and measured (experimental) values of gold adsorption rate.

Std	Run	A:mass of adsorbent (g)	B:contact time (min)	C:Temperature (°C)	D: Agitation (rpm)	gold uptake (%)
30	1	1.05	90	56	45	87.23
9	2	0.6	60	39	50	32.29
23	3	1.05	90	56	35	84.34
13	4	0.6	60	73	50	29.94
12	5	1.5	120	39	50	86.24
14	6	1.5	60	73	50	80.14
17	7	0.15	90	56	45	19.22
24	8	1.05	90	56	55	86.19
16	9	1.5	120	73	50	83.69
26	10	1.05	90	56	45	79.75
8	11	1.5	120	73	40	84.56
25	12	1.05	90	56	45	80.25
1	13	0.6	60	39	40	36.23
29	14	1.05	90	56	45	84.35
18	15	1.95	90	56	45	87.36
22	16	1.05	90	90	45	64.32
10	17	1.5	60	39	50	77.82
2	18	1.5	60	39	40	79.29
20	19	1.05	150	56	45	86.74
19	20	1.05	30	56	45	69.42
6	21	1.5	60	73	40	80.11
28	22	1.05	90	56	45	84.81
15	23	0.6	120	73	50	48.31
11	24	0.6	120	39	50	52.14
3	25	0.6	120	39	40	54.86
7	26	0.6	120	73	40	49.54
21	27	1.05	90	22	45	52.34
4	28	1.5	120	39	40	89.24
5	29	0.6	60	73	40	29.42
27	30	1.05	90	56	45	87.92

The model's adequacy and significance, as well as the effects of the elements, were assessed using the ANOVA (TABLE 4). The ANOVA showed that the equation accurately captured the true connection between the significant factors and the percentage of gold uptake. The model was likely significant based on the F value of 25.86. The model is sufficient for forecasting the adsorption rate of gold, as evidenced by the low F and high P ($P > 0.05$) values of lack of fit. Additionally, there is less than a 0.2 discrepancy between the Adjusted R^2 of 0.9231 and the Predicted R^2 of 0.7896. The signal to noise ratio is measured by Adeq Precision.

3.2. Influence of factors on gold uptake and 3D response surface plot

Figure 1 shows the perturbation plot of the primary factors' impact on the gold adsorption rate. At a specific location in the design space, these graphs help compare the effects of all the parameters. Figure 1 shows that the important factors are ranked as follows: A > B > C > D.

The 3D response surface plots shown in Figure 2 provide a clearer picture of the parameters influencing the uptake of gold.

Table 4: ANOVA results of quadratic model to predict the adsorption of gold on sugarcane bagasse

Source	Sum of Squares	df	Mean Square	F-value	p-value	
Model	13261.12	14	947.22	28.31	< 0.0001	significant
A-Mass	8995.43	1	8995.43	268.87	< 0.0001	
B-Time	793.27	1	793.27	23.71	0.0002	
C-temp.	0.1014	1	0.1014	0.0030	0.9568	
D-Agitation	3.36	1	3.36	0.1004	0.7557	
AB	160.02	1	160.02	4.78	0.0450	
AC	12.64	1	12.64	0.3777	0.5480	
AD	0.2652	1	0.2652	0.0079	0.9302	
BC	6.71	1	6.71	0.2005	0.6607	
BD	0.5476	1	0.5476	0.0164	0.8999	
CD	5.74	1	5.74	0.1714	0.6847	
A^2	2121.66	1	2121.66	63.42	< 0.0001	
B^2	185.06	1	185.06	5.53	0.0328	
C^2	1557.29	1	1557.29	46.55	< 0.0001	
D^2	17.61	1	17.61	0.5263	0.4793	
Residual	501.85	15	33.46			
Lack of Fit	443.16	10	44.32	3.78	0.0777	not significant
Pure Error	58.69	5	11.74			
Cor Total	13762.97	29				

This plot, which shows the link between two factors while keeping the other two at their central level for the gold uptake rate, reveals the main impact of the four elements. Figures 2 (a, b, and c) make it clear that as adsorbent mass and adsorption duration increase, the gold adsorption rate rises dramatically and linearly. The graphs in Figures 2 (a, d) similarly show that as contact duration increases, the adsorption rate first rises quickly before increasing more gradually. This behavior may result from the gel's high accessible surface area and vacant sites, which raise the driving force and interface. This is in tandem with the observations made in [14], where residuals buckwheat hulls was used in gold adsorption. Additionally, Fig. 2 shows that the absorbent's mass is the most important aspect and plays a significant influence in the sorption process (Fig. 2(a, b, and c)). Their adsorption rate increased in proportion to an increase in the adsorbent dosage. This may also be because increased adsorbent dosage catalyzes increased adsorbent uptake. This observation is in line with [15] where the behavior of gold adsorption from cyanide leaching solution onto activated coconut shell carbon was studied. It was observed that activated carbon is the most influential factor and has a major role on the sorption process.

3.3. Optimization

To achieve the maximum adsorption, the adsorption performance of gold from the aqua regia leaching solution was optimized using Design Expert software. The trend of factors for moving toward the ideal point is shown in Figure 3. The ideal process parameters were 1.4 g of adsorbent mass, 99 minutes of contact time, 60°C, and 45 rpm of agitation. In these circumstances, gold's adsorption effectiveness was roughly 91.5%. Three confirmation tests were conducted under the anticipated ideal conditions to verify the model's validity. In contrast to the adsorption rate of 91.5% determined by the model, the confirmatory studies revealed an adsorption efficiency of gold utilizing the produced gel (90%) under ideal conditions. Additionally, studies utilizing activated carbon of analar grade showed that, under ideal circumstances, gold adsorption effectiveness on activated carbon may reach almost 93.25%.

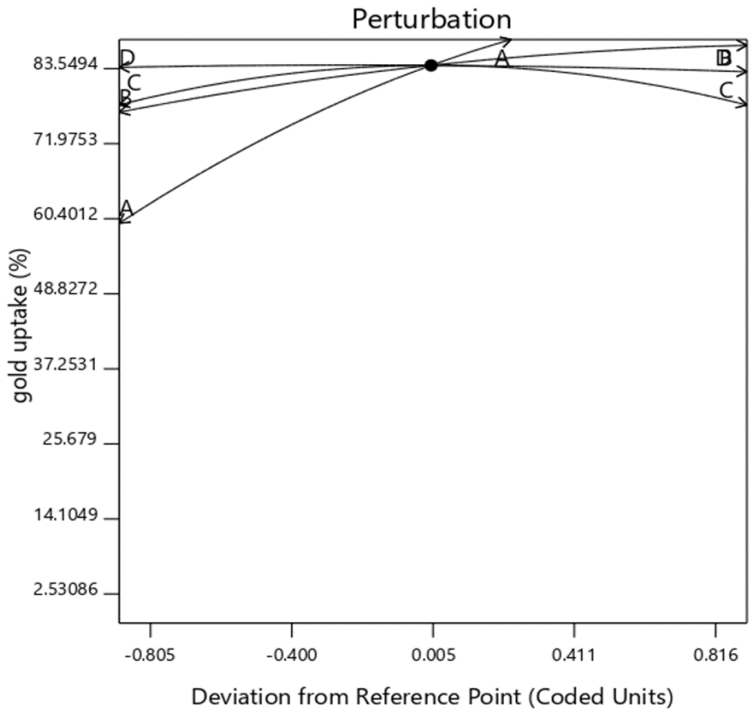

Figure 1: Perturbation plot showing the relative significance of factors on Au uptake percentage.

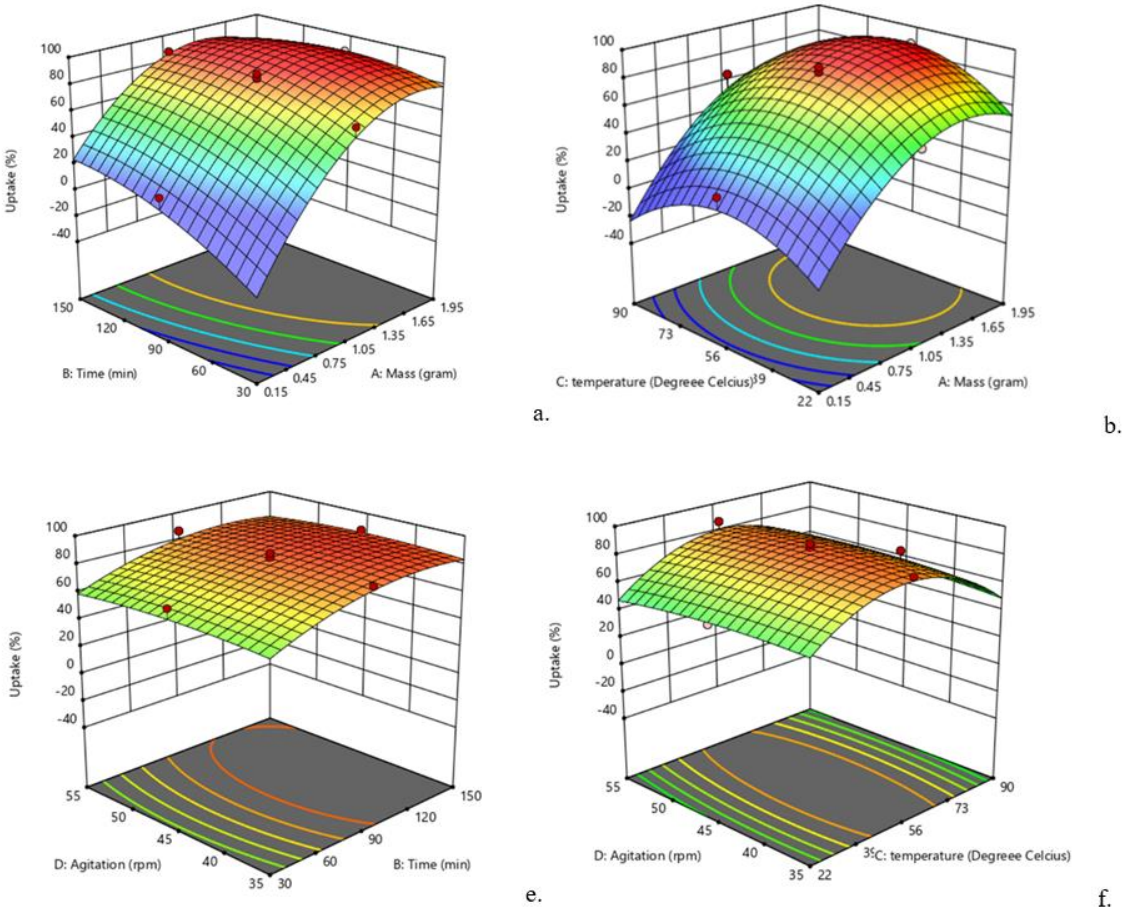

Figure 2: 3D response surface plots showing the effect of two factors on the adsorption rate of gold: (a) contact time and mass of adsorbent; (b) Temperature and mass of adsorbent; (c) agitation rate and mass of adsorbent; (d) Temperature and the contact time; (e) agitation rate and contact time (f) agitation rate and temperature.

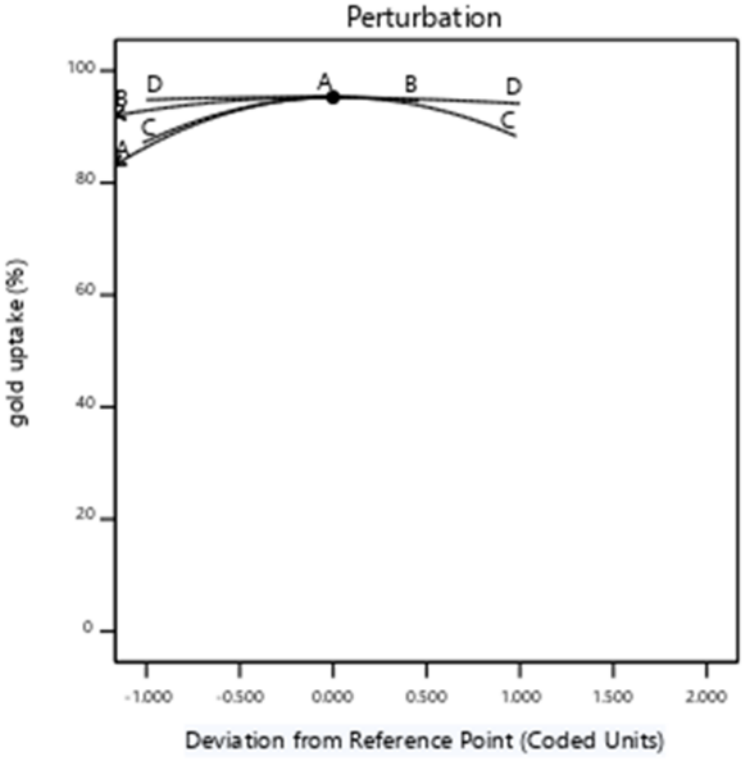

Figure 3: Perturbation plot showing the optimal conditions of factors to obtain the maximum adsorption rate on gel from sugarcane bagasse.

3.4. Adsorption Isotherm

The equilibrium sorption of Au(III) ions was achieved by stirring 10 mg of sugarcane bagasse nanocellulose with 10 ml of gold leachate of different Au(III) concentrations of 10, 20, 30, 40, and 50 mg/L in an Erlenmeyer flask at optimal temperatures of 323K. The results are shown in TABLE 5 and were fitted into the following isotherms: Langmuir, Freundlich, and Temkin. The Langmuir adsorption isotherm provides a quantitative explanation for the creation of an adsorbate monolayer on the adsorbent's outer surface, following which additional adsorption ceases. Langmuir adsorption parameters can be obtained by converting the equation into linear form.

$$\frac{C_e}{q_x} = \frac{C_e}{q_m} + \frac{1}{q_m K_L} \qquad (4)$$

The values of q_m and K_L were computed from the slope and intercept of the Langmuir plot of C_e/q_x versus C_e (Fig. 4a)

The essential characteristic of Langmuir isotherm is expressed by a dimensionless constant separation R_L, defined by:

$$R_L = \frac{1}{(1 + K_L C_o)} \qquad (5)$$

where, Co (mg /L) is the lowest initial concentration of gold solution. The RL values indicate the sorption to be either irreversible (RL = 0), favorable ($0 < R_L < 1$), linear ($R_L = 1$) or unfavorable ($R_L > 1$ or $R_L < 0$) [16].

Adsorption onto a heterogeneous surface through a multilayer adsorption mechanism is described by The Freundlich isotherm [17] the adsorption of gold(III) onto bagasse gel was subjected to the Freundlich model in its linear form:

$$log q_x = log\, k_f + {}^{1}/_{c_i}\, log\, c_e \qquad (6)$$

The values k_f and c_i for the respective temperatures were calculated from the intercept and slope of the linear plot between log q_x and log c_e (Fig. 4b). It has been reported that when $1< c_i < 10$, the adsorption is favorable, and the higher the ci value, the stronger the adsorption intensity [17].

The Temkin isotherm assumes that the heat of adsorption decreases linearly versus coverage rather than logarithmically, as for the Freundlich equation [18]. The equation describing this isotherm is expressed linearly as follows

$$q_x = \frac{RT}{\beta} lnk_t + \frac{RT}{\beta} lnc_e \qquad (7)$$

where R is the gas constant (0.0083 kJ mol^{-1} K^{-1}), T is the absolute temperature (K), β is the Temkin constant related to heat of adsorption (kJ mol^{-1}), and k_t is the Temkin isotherm constant (L g^{-1}). Parameters k_t and β were estimated by plotting the variation of q_x against ln c_e (Fig. 4c)

TABLE 5: Parameters for plotting Langmuir, Freundlich and Temkin Adsorption Isotherms obtained at 303K

C_o (mg/L)	C_e (mg/L)	$C_o - C_e$	$q_x=(C_o - C_e)*V/m$	Log C_e	Ln C_e	Log q_x	C_e/q_x
10	6.32	3.68	3.68	0.801	1.844	0.693	1.717
20	15.07	4.93	4.93	1.178	2.713	0.693	3.057
30	24.24	5.76	5.76	1.385	3.188	0.760	4.208
40	33.11	6.89	6.89	1.520	3.500	0.838	4.805
50	43.12	6.88	6.88	1.635	3.764	0.838	6.267

Table 6 displays the parameters obtained from the several projected graphs for the Freundlich, Temkin, and Langmuir isotherms. The adsorption of gold onto bagasse gels follows the Langmuir model preferentially at 333K, according to a comparison of the R2 values corresponding to the assessed isotherms. Additionally, the Langmuir model's RL values, which lie between 0 and 1, strongly suggested that gold sorption was favorable. According to the Freundlich model, the ci values for gold sorption at the temperature under consideration essentially fall between 1 and 10, indicating favorable sorption. Nevertheless, a moderate adsorption intensity was predicted because the value is less than 4.

TABLE 6: Parameters evaluated by using various isotherms for gold ion adsorption onto bagasse nanocellulose

Isotherm type	Parameters	323K
Langmuir	q_m	9.8039
	K_L	0.1048
	R^2	0.9772
	R_L	0.2413
Freundlich	k_f	2.431
	c_i	3.112
	R^2	0.983
Temkin	β (kJ/mol)	1.388
	k_t	1.461
	R^2	0.953

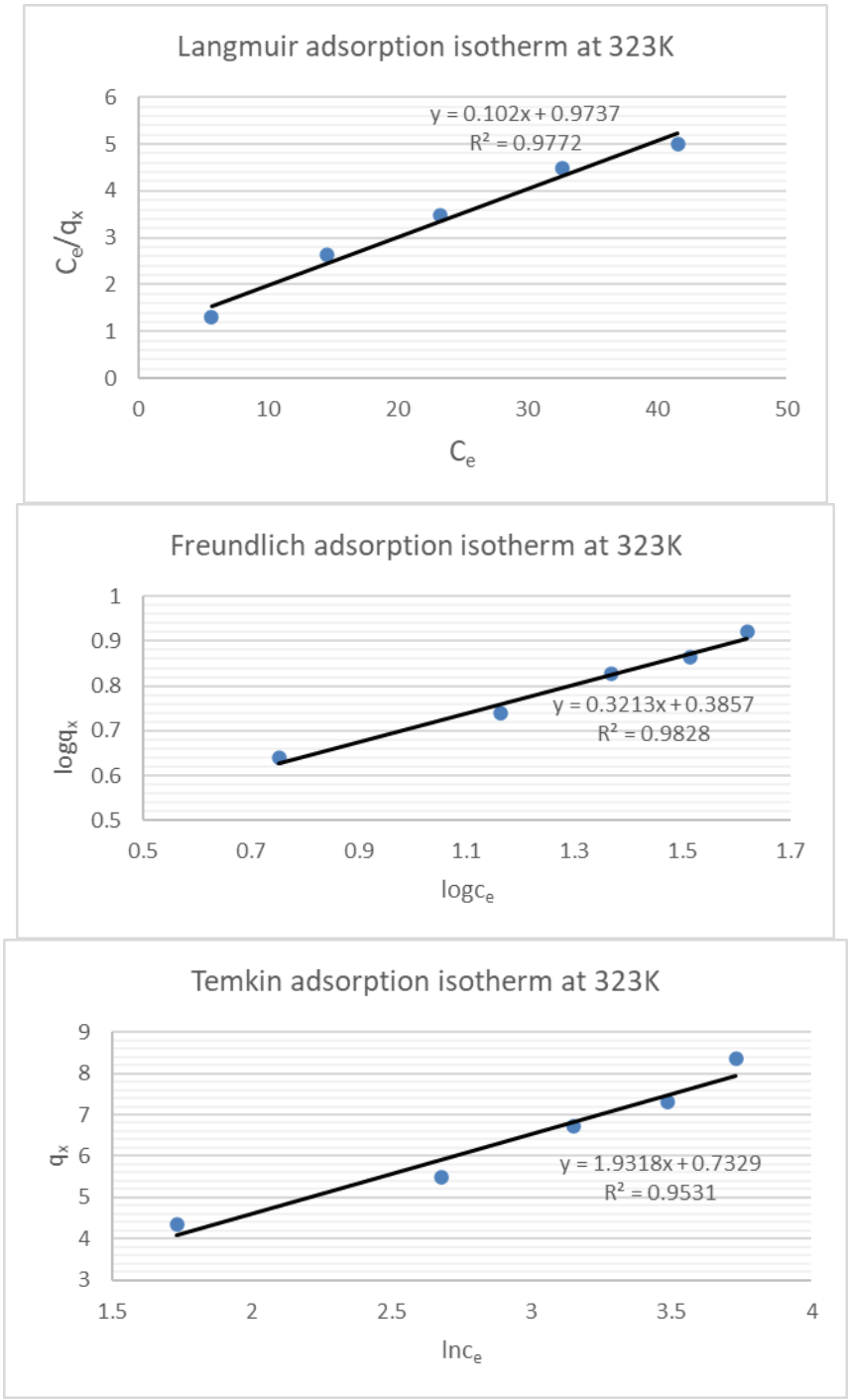

Figure 4: (a) Langmuir, (b) Freundlich and (c) Temkin isotherm for gold adsorption at 323K

4. CONCLUSION

Gold adsorption from leachate obtained from aqua-regia leached solution on gel formed from sugarcane bagasse ash has been investigated in relation to experimental factors such as mass of adsorbent, contact time, temperature, and agitation rate. These crucial elements were modeled and optimized using central composite design using response surface approach. A second-order quadratic model was constructed to characterize the behavior of the adsorption process. The significance of independent factors was examined using analysis of variance (ANOVA). ANOVA analysis showed that the most significant factors in the uptake of gold from aqua-regia leaching solution were the linear influence of bagasse dosage, the linear effect of contact time, the quadratic effect of adsorbent dosage, and the quadratic effect of temperature. The optimal parameters for the agitation rate, adsorbent dosage, temperature, and contact duration were determined to be 45 rpm, 1.4 g/L, 99 min, and 60°C, respectively. It was discovered that the adsorption yield was 91.5%. This improved value was confirmed and successfully compared to the yield of 93.25% that was obtained with activated carbon of

analar grade. Additionally, three isotherm models were used to derive and examine the adsorption equilibrium values. The fitted isotherms were ranked as follows: Langmuir > Freundlich > Temkin.

ACKNOWLEDGEMENT
The authors acknowledge the support of the Department of Materials Science and Engineering of Obafemi Awolowo University, Ile Ife, Nigeria as well as the Department of Chemical and Petroleum Engineering of Abiola Ajimobi Technical University, Ibadan, Nigeria.

REFERENCES

[1] Malitch, K.N., Lipenkov, G.V., Ozornin, D.A. (2024). Gold Mineralzation from Calcite-Dolomite Carbonatite of the Guli Massif (Maimecha-Kotui Province, Polar Siberia): First Results. Dokl. Earth Sc. 519, 1899–1905. https://doi.org/10.1134/S1028334X24603079

[2] Hammer, V., Vanneste, J., Vuono, D., Alejo-Zapata, F., Polanco-Cornejo, H., Zea, J., Sosa, H., Rojas, C., Figueroa, L. and Bellona, C. (2023). Membrane Contactors as a Cost-Effective Cyanide Recovery Technology for Sustainable Gold Mining. ACS ES&T Water. 3. 10.1021/acsestwater.3c00026.

[3] Teniola, O. S., Adeleke, A. A., Ibitoye, S. A., & Shitu, M. D. (2022). Leaching of a Nigerian refractory gold ore using aqua regia. *American Journal of Engineering and Applied Sciences*, *15*(1), 118-125.

[4] Seydou D., Ata A. and Sandeep P., (2025). Study of alkaline hydrometallurgical process for stibnite flotation tailings reprocessing: Semi-pilot antimony leaching, Minerals Engineering, Vol. 222,109168,ISSN 0892-6875,https://doi.org/10.1016/j.mineng.2024.109168.

[5] Inoue, K., Parajuli, D., Gurung, M., Pangeni, B., Khunathai, K., Ohto, K. and Kawakita, H. (2019). Gold Recovery Process from Primary and Secondary Resources Using Bioadsorbents. DOI: http://dx.doi.org/10.5772/intechopen.84770.

[6] Teniola, O., Ibitoye, S., & Adeleke, A. (2016). Multistage Mineral Acid Leaching De-Mineralization of a Medium Caking Coal. Ife Journal of Technology, 24(1), 6–10. Retrieved from https://ijt.oauife.edu.ng/index.php/ijt/article/view/17

[7] Barnov, N.G., Lavrinenko, A.A., Lusinyan, O.G. (2018). Effect of a Crushing Technique on Lead–Zinc Ore Processing Performance. *J Min Sci* **53**, 771–777. https://doi.org/10.1134/S1062739117042765

[8] Tiza, M., Okafor, F. and Agunwamba, J. (2025). Energy dispersive X-Ray fluorescence (EDXRF)-oxide composition analysis of coarse aggregates and reclaimed asphalt pavement (RAP)as construction materials. Journal of Polytechnic, 28(3) : 785-801

[9] Tang, Y., Yin, W., Huang, S., Xue, J. and Zuo, W., (2020). Enhancement of gold agitation leaching by HPGR comminution via microstructural modification of gold ore particles, Minerals Engineering, Volume 159, 106639, ISSN 0892-6875, https://doi.org/10.1016/j.mineng.2020.106639.

[10] Adebisi, J. A., Agunsoye, J. O., Bello, S. A., Kolawole, F. O., Ramakokovhu, M. M., Daramola, M. O. and Hassan, S. B. (2017). Extraction of Silica from Sugarcane Bagasse, Cassava Periderm and Maize Stalk: Proximate Analysis and Physico-Chemical Properties of Wastes. Waste Biomass Valor DOI 10.1007/s12649-017-0089-5

[11] Pi X, Yao Y, Qin D, Liu T. (2025). Effect of gel ageing and electrode corrosion on the performance of direct laser writing carbonization-enabled hydrogel-based moist-electric generators. 5(23):18548-18558. doi:10.1039/d5ra02872h.

[12] Goharrizi, F.S., Ebrahimipour, S.Y., Ebrahimnejad, (2024). Magnetic Mesoporous Silica Functionalized with Amine Groups for Efficient Removal of Heavy Metals and Bacterial Inhibition. *J Clust Sci* **35**, 2419–2435 (2024). https://doi.org/10.1007/s10876-024-02669-y

[13] Elganidi, I., Elarbe, B. and Ridzuan, N. (2022). Optimisation of reaction parameters for a novel polymeric additives as flow improvers of crude oil using response surface methodology. *J Petrol Explor Prod Technol* **12**, 437–449. https://doi.org/10.1007/s13202-021-01349-1

[14] Kun, D., Ping, Y., Xiguang, L., Qinghua, T., and Rongjun, Q., (2014). Modeling, analysis and optimization of adsorption parameters of Au(III) using low-cost agricultural residuals buckwheat hulls, Journal of Industrial and Engineering Chemistry, Volume 20, Issue 4, Pages 2428-2438, ISSN 1226-086X, https://doi.org/10.1016/j.jiec.2013.10.023.

[15] Khosravi, R., Azizi, A., Ghaedrahmati, R, Gupta, V. and Agarwal, S. (2017). Adsorption of gold from cyanide leaching solution onto activated carbon originating from coconut shell—Optimization, kinetics and equilibrium studies. Journal of Industrial and Engineering Chemistry. 54. 10.1016/j.jiec.2017.06.036.

[16] Du, J., Xiao, J., Ma, X. and Li, J. (2026). Crown ether-functionalized polyimide nanofiber membranes fabricated by in-situ grafting and electrospinning for efficient selective adsorption of cesium, Desalination, Volume 618, 2026, 119445, ISSN 0011-9164, https://doi.org/10.1016/j.desal.2025.119445.

[17] Wagassa, A. N., Zereffa, E. A., Shifa, T. A. and Bansiwal, A. (2026). Synthesis and Characterization of Mn-Doped Ni–Al Layered Double Oxides Nanoplates for Fluoride Adsorption: Studies on Adsorption Isotherms, Kinetics, Thermodynamics and Regeneration. Water, Air, & Soil Pollution. 237. 10.1007/s11270-026-09129-5.

[18] Al-Rashdi, K.S., Elzain, M.E., Al-Barwani, M.S., Moore, E.A and Widatallah, H.M. (2023). Computational modeling of the defect structure, hyperfine and magnetic properties of the Mn2+-doped magnetite of the composition MnxFe3-yO4 (y = ⅔ x), Materials Research Bulletin, Volume 159, 2023, 112095, ISSN 0025-5408, https://doi.org/10.1016/j.materresbull.2022.112095.